

Consistent description of the electronic structure of SrVO₃ within *GW*+DMFT

R. Sakuma,¹ Ph. Werner,² and F. Aryasetiawan¹

¹*Department of Physics, Division of Mathematical Physics,
Lund University, Sölvegatan 14A, 223 62 Lund, Sweden*

²*Department of Physics, University of Fribourg, 1700 Fribourg, Switzerland*

(Dated: August 14, 2019)

We present a detailed calculation of the electronic structure of SrVO₃ based on the *GW*+DMFT method. We show that a proper inclusion of the frequency-dependent Hubbard *U* and the non-local self-energy via the *GW* approximation, as well as a careful treatment of the Fermi level, are crucial for obtaining an accurate and coherent picture of the quasi-particle band structure and satellite features of SrVO₃. The *GW*+DMFT results for SrVO₃ are not attainable within the *GW* approximation or the LDA+DMFT scheme.

PACS numbers: 71.20.-b, 71.27.+a

Describing the electronic structure of correlated materials fully from first principles is one of the great challenges in modern condensed matter physics. The dynamical mean-field theory (DMFT)¹⁻³ in combination with the local density approximation (LDA), known as the LDA+DMFT scheme,⁴⁻⁷ has in many cases provided a realistic description of the electronic structure and spectral functions of correlated materials. This method, however, suffers from a number of conceptual problems. One of them is the double-counting problem that arises from the difficulty in subtracting the contribution of the LDA exchange-correlation potential in the correlated subspace. Another shortcoming is the DMFT assumption that the self-energy is local. A recent study based on the *GW* approximation (GWA)⁸⁻¹¹ indicates that even in correlated materials, such as SrVO₃, the non-local self-energy has a non-negligible influence on the electronic structure. In particular, it was found that the non-local self-energy widens the bandwidth significantly.¹²

A decade ago, a different first-principle scheme was proposed, which combines the GWA and the DMFT. This *GW*+DMFT scheme¹³ has the potential of curing the main shortcomings of both the GWA and the DMFT. It goes beyond the GWA by including onsite vertex corrections via the DMFT. Alternatively, from the DMFT point of view, the scheme incorporates a nonlocal self-energy via the GWA. *GW*+DMFT calculations are fully first principles and self-contained in the sense that the Hubbard *U* needed in DMFT can in principle be determined self-consistently. Moreover, they do not suffer from the double-counting problem.

In the present work, we apply the *GW*+DMFT scheme to the much studied cubic perovskite SrVO₃, generally considered to be a prototype of correlated metals, as is evident from the large number of both experimental¹⁴⁻²² and theoretical works.²³⁻³¹ Experimentally, a substantial *t_{2g}* band narrowing by a factor of two compared with the LDA bandwidth is observed.²⁰ In addition, there are satellite features a few eV below and above the Fermi level, interpreted as the lower and upper Hubbard bands.^{14-16,20} Intriguing kinks at low energies are also observed in photoemission experiments.²²

A consistent and coherent description of the electronic structure of SrVO₃ that reproduces all these features provides a stringent test for first-principles schemes, since both the satellite features *and* the quasi-particle band structure must be correctly described. LDA+DMFT calculations with a static *U* yield a band narrowing by a factor of two if a large value of *U* = 5.5 eV is used,²⁷ but this results in a too large separation of the Hubbard bands.²⁶ Recent *GW* calculations on the other hand yield neither the correct band narrowing nor a correct description of the Hubbard bands¹² even when the so-called quasi-particle self-consistent *GW* scheme is employed.³² This indicates that vertex corrections beyond the GWA must be included, as supported also by a recent study on the α - γ transition in cerium.³³

Applications of the *GW*+DMFT method are rather scarce and the existing works^{34,35} have focused mainly on the spectral functions and Hubbard bands, which are essentially determined by *U*, whereas little attention has been paid to the quasi-particle band structure, which depends on precise details of the self-energy. Moreover, Ref. 35 used a static *U* rather than a frequency-dependent *U*. Applications to a Hubbard model³⁶ and to surface systems within tight-binding model³⁷ have also been carried out. Here, we will demonstrate that both the frequency-dependent *U* *and* the nonlocal self-energy, as well as a careful treatment of the chemical potential, are essential for obtaining an accurate and coherent description of the electronic structure of SrVO₃ entirely from first principles. The picture that emerges is distinct from either the pure *GW* or the DMFT pictures and thus reveals the importance of the nonlocal self-energy, missing in the DMFT treatment, and the onsite vertex corrections, which are missing in the GWA.

*The *GW*+DMFT method.* The *GW*+DMFT method was proposed in Ref. 13 and may be implemented at various levels of self-consistency. Here we describe the scheme in its simplest form, the one used in the present work. Progress in solving the DMFT impurity problem with dynamic *U* by means of continuous-time Quantum Monte Carlo (CT-QMC) methods³⁸⁻⁴² has made a proper implementation of the *GW*+DMFT scheme pos-

sible. Our calculations are based on the strong-coupling CT-QMC technique explained in Refs. 41 and 43.

In the GW +DMFT scheme the total self-energy is given by the sum of the GW self-energy and the DMFT impurity self-energy with a double-counting correction:

$$\hat{\Sigma}(\omega) = \sum_{\mathbf{k}nn'} |\psi_{\mathbf{k}n}\rangle \Sigma_{nn'}^{GW}(\mathbf{k}, \omega) \langle \psi_{\mathbf{k}n'} | \\ + \sum_{mm'} |\varphi_m\rangle \left[\Sigma_{mm'}^{\text{imp}}(\omega) - \Sigma_{mm'}^{\text{DC}}(\omega) \right] \langle \varphi_{m'} |, \quad (1)$$

where $\{\psi_{\mathbf{k}n}\}$ is the LDA Bloch states and the $\{\varphi_m\}$ are the Wannier orbitals constructed from the vanadium t_{2g} bands. The GW self-energy and the impurity self-energy are calculated separately, the latter is obtained from the LDA+DMFT scheme with dynamic U . The double-counting correction Σ^{DC} is the contribution of Σ^{GW} to the onsite self-energy which is already contained in the impurity self-energy Σ^{imp} calculated within the DMFT with dynamic U . The explicit formula for the double-counting correction is

$$\Sigma_{mm'}^{\text{DC}}(\omega) = i \sum_{m_1 m_2 C t_{2g}} \int \frac{d\omega'}{2\pi} G_{m_1 m_2}^{\text{loc}}(\omega + \omega') \\ \times W_{m m_1, m_2 m'}^{\text{loc}}(\omega'), \quad (2)$$

where $G^{\text{loc}}(\omega) = \sum_{\mathbf{k}} S^\dagger(\mathbf{k}) G(\mathbf{k}, \omega) S(\mathbf{k})$ is the onsite projection of the lattice Green function of the t_{2g} subspace, with $S(\mathbf{k})$ the transformation matrix that yields the maximally localized Wannier orbitals according to the prescription of Marzari and Vanderbilt.^{45,46} We employ a recently proposed symmetry-constrained routine⁴⁷ to construct symmetry-adapted Wannier functions using a customized version of the Wannier90 library.⁴⁸ The matrix elements of W^{loc} are

$$W_{m m_1, m_2 m'}^{\text{loc}}(\omega) = \int d^3 r d^3 r' \varphi_m^*(\mathbf{r}) \varphi_{m_1}(\mathbf{r}) W^{\text{loc}}(\mathbf{r}, \mathbf{r}'; \omega) \\ \times \varphi_{m_2}^*(\mathbf{r}') \varphi_{m'}(\mathbf{r}'), \quad (3)$$

and W^{loc} is obtained from

$$W^{\text{loc}}(\omega) = [1 - U^{\text{loc}}(\omega) P^{\text{loc}}(\omega)]^{-1} U^{\text{loc}}(\omega). \quad (4)$$

Here, U^{loc} is the onsite Hubbard U of the impurity problem calculated using the constrained random-phase approximation (cRPA)⁴⁹ and $P^{\text{loc}} = -iG^{\text{loc}}G^{\text{loc}}$ is the local polarization for each spin channel. The quasi-particle band structure is obtained from the solution of

$$E_{\mathbf{k}n} - \varepsilon_{\mathbf{k}n} - \text{Re}\Sigma_{nn}(\mathbf{k}, E_{\mathbf{k}n}) = 0. \quad (5)$$

In this work, the LDA and GW calculations have been performed using the full-potential linearized augmented plane-wave codes FLEUR and SPEX.⁴⁴

Quasi-particle band structure. Angle-resolved photoemission (ARPES) measurements reveal a clear t_{2g} quasi-particle band dispersion and a broad almost structureless incoherent feature centered at -1.5 eV below the

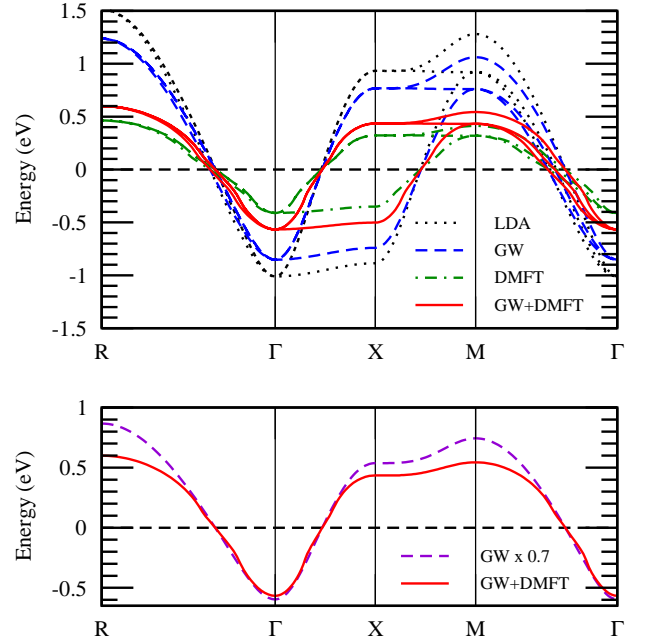


FIG. 1: (color online). Upper panel: the quasi-particle band structure of SrVO_3 within LDA, GW , DMFT, and GW +DMFT. Lower panel: To emphasize the kink structure near Γ , the GW +DMFT band is plotted against a renormalized GW band.

Fermi level.²⁰ A mass enhancement by a factor of 2 near the Fermi level is observed²⁰ consistent with the electronic specific-heat coefficient γ within the Fermi-liquid picture.¹⁵

In Fig. 1 we present the quasi-particle band structure obtained from several approaches. The band width within LDA, GW , DMFT, and GW +DMFT are respectively 2.6, 2.1, 0.9, and 1.2 eV. From the measured effective mass of 2 with respect to the LDA, one may infer that the experimental bandwidth should be approximately 1.3 eV. Upon inclusion of the self-energy correction within the GWA, the LDA band is narrowed to 2.1 eV, which is still much too wide in comparison with the experimental value. The DMFT quasi-particle bandwidth is 0.9 eV, which is too narrow compared to experiment. As pointed out in an earlier work¹² the nonlocal self-energy tends to widen the band. Indeed, when the nonlocal self-energy is taken into account within the GW +DMFT scheme, the DMFT bandwidth increases to 1.2 eV, in good agreement with the experimental result. Starting from the GW band, the result may also be interpreted as a band narrowing due to onsite vertex corrections.⁵⁰ Since little experimental data is available for the unoccupied part of the band it may be more reliable to compare the occupied part of the calculated band with experiment. From ARPES data²⁰ the bottom of the occupied band is within -0.7 eV, which is to be compared with -0.6 eV in GW +DMFT whereas the corresponding values for LDA, GW , and DMFT are respectively -1.0 , -0.9 , and

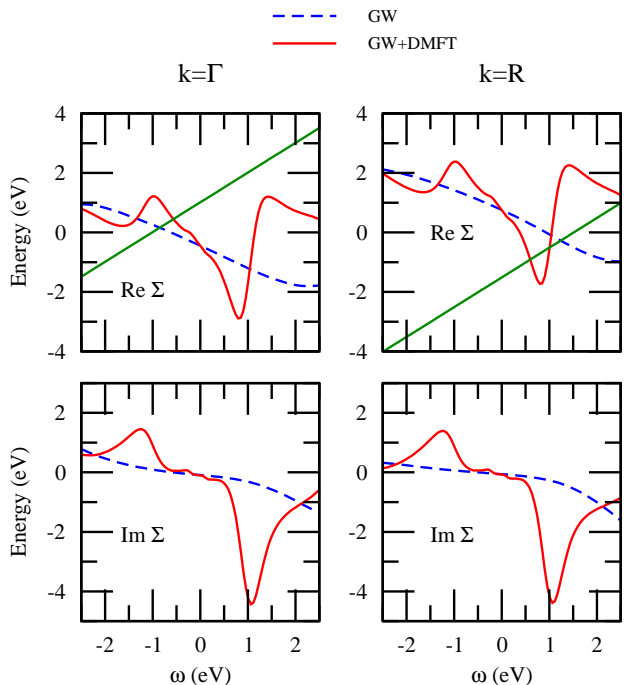


FIG. 2: (color online). GW and $GW+DMFT$ self-energies at the Γ - and R -points. The straight line is $\omega - \varepsilon_{\mathbf{k}n}$ where $\varepsilon_{\mathbf{k}n}$ is the LDA energy.

-0.4 eV, as can be seen in Fig. 1.

Kinks. Intriguing kink features in the band dispersion were recently observed: a sharp kink at ~ 60 meV, likely of phonon origin, and a broad high-energy kink at ~ 0.3 eV below the Fermi level.²² Since SrVO_3 is a Pauli-paramagnetic metal without any signature of magnetic fluctuations, the presence of a kink at high energy suggests a mechanism which is not related to spin fluctuations. Previous calculations based on the LDA+DMFT scheme explained the high-energy kink as purely of electronic origin.²⁷ We also observe visible broad kinks between -0.1 and -0.4 eV in the vicinity of the Γ -point in the $GW+DMFT$ band structure as can be seen in the lower panel of Fig. 1, where one of the $GW+DMFT$ bands is plotted against a renormalized GW band, as was similarly done in Ref. 27. The broad kinks can be recognized as deviations from a parabolic band. The origin of these kinks may be traced back to the deviation from a linear behavior of $\text{Re}\Sigma$ between -0.5 and $+0.5$ eV as may be seen in Fig. 2. As we scan the straight line $\omega - \varepsilon_{\mathbf{k}n}$ from the Γ -point along $\Gamma - R$ or $\Gamma - X$, the crossing with $\text{Re}\Sigma$, which is the position of the quasi-particle, experiences an oscillation resulting in a kink in the quasi-particle dispersion.

Static vs dynamic U . The major effect of the dynamic U is the reduction in the quasi-particle weight or the Z -factor, as can be inferred from the slope of the Matsubara-axis self-energy at $\omega = 0$ [$Z \approx 1/(1 - \text{Im}\Sigma(i\omega_0)/\omega_0)$], which is larger in the dynamic than the

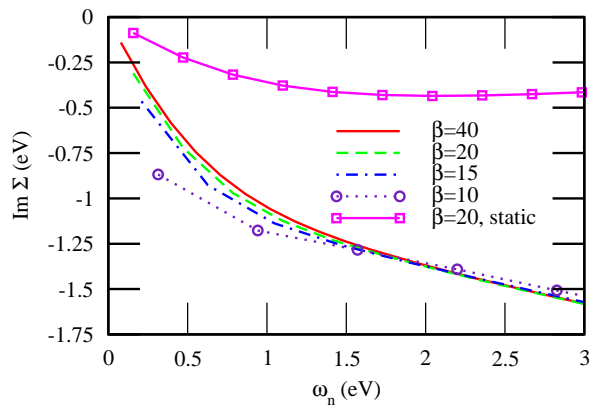


FIG. 3: (color online). The imaginary part of the self-energy for a range of inverse temperatures β along the Matsubara axis for dynamic U . The result for static U is also shown for $\beta = 20$. The unit of β is eV^{-1} .

static U case (Fig. 3). This reduction in the quasi-particle weight is due to the coupling to the high-energy plasmon excitations, missing in the static U calculation. In Fig. 3 we can also see the dependence of the DMFT self-energy on temperature. As the temperature is increased the system starts to deviate from Fermi liquid behavior. It would be interesting to see if this theoretical prediction can be observed experimentally.

The reduction in the Z -factor due to the dynamic U results in a band narrowing. This band narrowing has been interpreted in a previous work⁵² as the result of a two-step process: first the high-energy part of U renormalizes the one-particle LDA band via the self-energy and then the remaining low-energy U , which is approximately the static U , renormalizes these bands further, so that the final bandwidth is significantly narrower than the one obtained from just the static U . It was then argued that in order to obtain the same band narrowing as in the full calculation with dynamic U , the starting bandwidth should be reduced if the static cRPA U is to be used.⁵² Indeed, to achieve the experimentally observed band narrowing a larger static U (~ 5 eV), compared with the static cRPA U of 3.4 eV, is needed in DMFT calculations. The larger static U however leads to an inconsistency: while the band narrowing or the mass enhancement is correct, the separation of the Hubbard bands becomes too large.^{26,34} For example, the lower Hubbard band came out too low at ~ -2.5 eV.^{26,27} The $GW+DMFT$ total spectral function is shown in Fig. 4 where a broad lower Hubbard band is found centered at -1.5 eV, in agreement with a recent photoemission data by Yoshida et al²⁰. No conclusive data are available for the upper Hubbard band but our theoretical calculation predicts its position at about 2 eV above the Fermi level.

From Fig. 2 it can be inferred that the lower Hubbard band corresponding to the occupied state at the Γ -point has higher intensity than the one corresponding to the

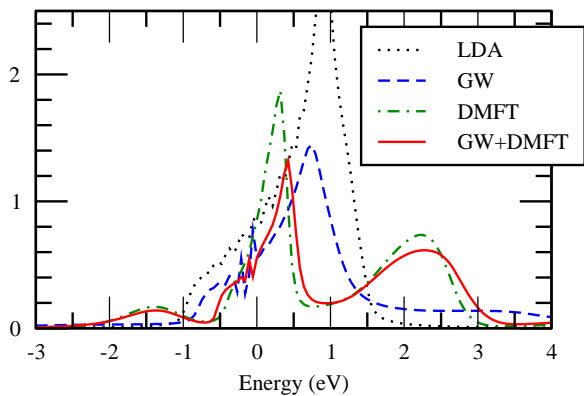


FIG. 4: (color online). The total spectral function within LDA, GWA, DMFT, and $GW+DMFT$.

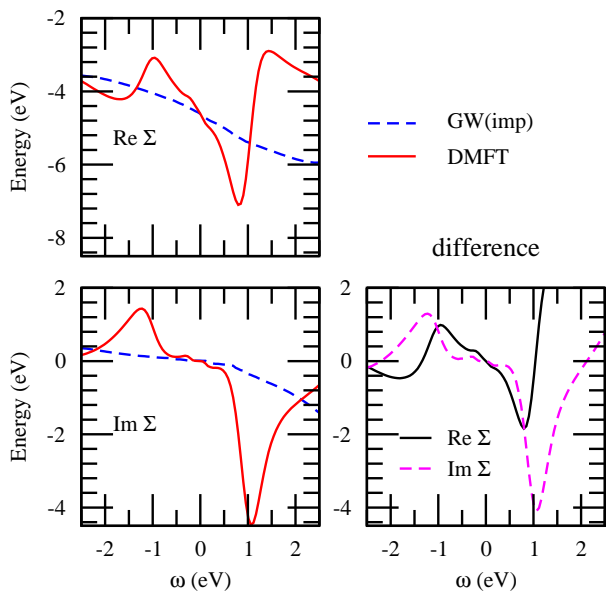


FIG. 5: (color online). The DMFT and GW impurity self-energies and the vertex correction, which is the difference between the two self-energies.

unoccupied state at the R -point.²⁰ Conversely, the upper Hubbard band corresponding to the unoccupied state at the R -point is more prominent than the one corresponding to the occupied state at the Γ -point. Moreover, it is also clear that the position of the Hubbard band arising from the state at the Γ -point is at approximately 1.5 eV above the Fermi level, lower than the one arising from the state at the R -point, which lies at approximately 2.5 eV. Thus, there is a strong dispersion in the upper Hubbard

band.

Double-counting correction and vertex correction. In Fig. 5 we compare the DMFT and GW impurity self-energies. The two self-energies are aligned so that the difference in $\text{Re } \Sigma$ is zero at the Fermi level, because the GW self-energy has not been calculated self-consistently. This alignment is crucial to avoid a problem with negative spectral weight and to obtain a physically meaningful spectral function. The difference between the impurity self-energies obtained from the DMFT and the GWA, shown in the right hand panel of Fig. 5, may be regarded as an onsite vertex correction to the GW self-energy and it is at the heart of the $GW+DMFT$ scheme. It becomes evident that the vertex correction introduces on top of the GW self-energy a strong peak in $\text{Im } \Sigma$ at 1 eV and consequently a strong variation in $\text{Re } \Sigma$ leading to the formation of a satellite at about 2 eV above the Fermi level. On the other hand, we find a weaker peak in $\text{Im } \Sigma$ below the Fermi level and accordingly a broad incoherent structure in the spectral function (see Fig. 4) as found experimentally by Yoshida *et al.*²⁰

In summary, we have performed calculations of the quasi-particle band structure as well as the spectral function of SrVO_3 within a simple version of $GW+DMFT$. While the bottom of the occupied GW band is too deep (-0.9 eV) and the DMFT with dynamic U too high (-0.4 eV), the $GW+DMFT$ scheme yields a value of -0.6 eV, which is in good agreement with the experimental value of -0.7 eV. From the point of view of the GWA the result illustrates the importance of onsite vertex corrections whereas from the DMFT point of view it demonstrates the significance of the non-local self-energy. The $GW+DMFT$ scheme is sufficiently sensitive to yield kink structures in the quasi-particle dispersion between -0.1 and -0.4 eV in the vicinity of the Γ -point. A well-defined upper Hubbard band centered at around 2 eV is obtained whereas a rather broad incoherent feature is found below the quasi-particle peak centered at around -1.5 eV. Our calculations also predict deviations from Fermi liquid behavior as the temperature is increased above $T \gtrsim 0.1$.

Acknowledgments We would like to thank S. Biermann for careful reading of the manuscript and for many useful comments. We would also like to thank C. Friedrich and S. Blügel for providing us with their FLAPW code and M. Casula, and T. Miyake for fruitful discussions. This work was supported by the Swedish Research Council and “Materials Design through Computics: Complex Correlation and Non-Equilibrium Dynamics”, a Grant in Aid for Scientific Research on Innovative Areas, MEXT, Japan, and by the Scandinavia-Japan Sasakawa Foundation. PW acknowledges support from SNF Grant No. 200021_140648.

¹ W. Metzner and D. Vollhardt, Phys. Rev. Lett. **62**, 324 (1989).

² A. Georges and G. Kotliar, Phys. Rev. B **45**, 6479 (1992).

³ A. Georges, G. Kotliar, W. Krauth, and M. J. Rozenberg,

- Rev. Mod. Phys. **68**, 13 (1996).
- ⁴ V. I. Anisimov, A. I. Poteryaev, M. A. Korotin, A. O. Anokhin, and G. Kotliar, J. Phys. Cond. Matter **9**, 7359 (1997).
 - ⁵ A. I. Lichtenstein and M. I. Katsnelson, Phys. Rev. B **57**, 6884 (1998).
 - ⁶ G. Kotliar, S. Y. Savrasov, K. Haule, V. S. Oudovenko, O. Parcollet, C. A. Marianetti, Rev. Mod. Phys. **78**, 865 (2006).
 - ⁷ K. Held, Adv. Phys. **56**, 829 (2007).
 - ⁸ L. Hedin, Phys. Rev. **139**, A796 (1965).
 - ⁹ F. Aryasetiawan and O. Gunnarsson, Rep. Prog. Phys. **61**, 237 (1998).
 - ¹⁰ W. G. Aulbur, L. Jönsson, and J. W. Wilkins, Solid State Physics **54**, 1 (2000).
 - ¹¹ G. Onida, L. Reining, and A. Rubio, Rev. Mod. Phys. **74**, 601 (2002).
 - ¹² T. Miyake, C. Martins, R. Sakuma, and F. Aryasetiawan, Phys. Rev. B **87**, 115110 (2013).
 - ¹³ S. Biermann, F. Aryasetiawan, and A. Georges, Phys. Rev. Lett. **90**, 086402 (2003).
 - ¹⁴ K. Morikawa, T. Mizokawa, K. Kobayashi, A. Fujimori, H. Eisaki, S. Uchida, F. Iga, and Y. Nishihara, Phys. Rev. B **52**, 13711 (1995).
 - ¹⁵ I. H. Inoue, O. Goto, H. Makino, N. E. Hussey, and M. Ishikawa, Phys. Rev. B **58**, 4372 (1998).
 - ¹⁶ A. Sekiyama, H. Fujiwara, S. Imada, S. Suga, H. Eisaki, S. I. Uchida, K. Takegahara, H. Harima, Y. Saitoh, I. A. Nekrasov, G. Keller, D. E. Kondakov, A. V. Kozhevnikov, Th. Pruschke, K. Held, D. Vollhardt, and V. I. Anisimov, Phys. Rev. Lett. **93**, 156402 (2004).
 - ¹⁷ T. Yoshida, K. Tanaka, H. Yagi, A. Ino, H. Eisaki, A. Fujimori, and Z.-X. Shen, Phys. Rev. Lett. **95**, 146404 (2005).
 - ¹⁸ R. Eguchi, T. Kiss, S. Tsuda *et al*, Phys. Rev. Lett. **96**, 076402 (2006).
 - ¹⁹ M. Takizawa, M. Minohara, H. Kumigashira, D. Toyota, M. Oshima, H. Wadati, T. Yoshida, A. Fujimori, M. Lippmaa, M. Kawasaki, H. Koinuma, G. Sordi, and M. Rozenberg, Phys. Rev. B **80**, 235104 (2009).
 - ²⁰ T. Yoshida, M. Hashimoto, T. Takizawa, A. Fujimori, M. Kubota, K. Ono, and H. Eisaki, Phys. Rev. B **82**, 085119 (2010).
 - ²¹ K. Yoshimatsu, K. Horiba, H. Kumigashira, T. Yoshida, A. Fujimori, and M. Oshima, Science **333**, 319 (2011).
 - ²² S. Aizaki, T. Yoshida, K. Yoshimatsu, M. Takizawa, M. Minohara, S. Ideta, A. Fujimori, K. Gupta, P. Mahadevan, K. Horiba, H. Kumigashira, and M. Oshima, Phys. Rev. Lett. **109**, 056401 (2012).
 - ²³ K. Maiti, D. D. Sarma, M. J. Rozenberg, I. H. Inoue, H. Makino, O. Goto, M. Pedio, and R. Cimino, Europhys. Lett. **55**, 246 (2001).
 - ²⁴ A. Liebsch, Phys. Rev. Lett. **90**, 096401 (2003).
 - ²⁵ E. Pavarini, S. Biermann, A. Poteryaev, A. I. Lichtenstein, A. Georges, and O. K. Andersen, Phys. Rev. Lett. **92**, 176403 (2004).
 - ²⁶ K. Maiti, U. Manju, S. Ray, P. Mahadevan, I. H. Inoue, C. Carbone, and D. D. Sarma, Phys. Rev. B **73**, 052508 (2006).
 - ²⁷ I. A. Nekrasov, K. Held, G. Keller, D. E. Kondakov, Th. Pruschke, M. Kollar, O. K. Andersen, V. I. Anisimov, and D. Vollhardt, Phys. Rev. B **73**, 155112 (2006).
 - ²⁸ M. Karolak, T. O. Wehling, F. Lechermann, and A. I. Lichtenstein, J. Phys.: Condens. Matter **23**, 085601 (2011).
 - ²⁹ M. Casula, A. Rubtsov, and S. Biermann, Phys. Rev. B **85**, 035115 (2012).
 - ³⁰ H. Lee, K. Foyevtsova, J. Ferber, M. Aichhorn, H. O. Jeschke, and R. Valenti, Phys. Rev. B **85**, 165103 (2012).
 - ³¹ L. Huang and Y. Wang, Europhys. Lett. **99**, 67003 (2012).
 - ³² M. Gatti and M. Guzzo, Phys. Rev. B **87**, 155147 (2013).
 - ³³ R. Sakuma, T. Miyake, and F. Aryasetiawan, Phys. Rev. B **86**, 245126 (2012).
 - ³⁴ J. M. Tomczak, M. Casula, T. Miyake, F. Aryasetiawan, and S. Biermann, Europhys. Lett. **100**, 67001 (2012).
 - ³⁵ C. Taranto, M. Kaltak, N. Parragh, G. Sangiovanni, G. Kresse, A. Toschi, and K. Held, arXiv:1211.1324v1.
 - ³⁶ P. Sun and G. Kotliar, Phys. Rev. Lett. **92**, 196402 (2004).
 - ³⁷ P. Hansmann, T. Ayril, L. Vaugier, P. Werner, and S. Biermann, Phys. Rev. Lett. **110**, 166401 (2013).
 - ³⁸ A. N. Rubtsov, V. V. Savkin and A. I. Lichtenstein, Phys. Rev. B **72**, 035122 (2005).
 - ³⁹ P. Werner, A. Comanac, L. de' Medici, M. Troyer, A. J. Millis, Phys. Rev. Lett. **97**, 076405 (2006).
 - ⁴⁰ P. Werner, A. J. Millis, Phys. Rev. B **74**, 155107 (2006).
 - ⁴¹ P. Werner, A. J. Millis, Phys. Rev. Lett. **99**, 146404 (2007).
 - ⁴² F. F. Assaad and T. C. Lang, Phys. Rev. B **76**, 035116 (2007).
 - ⁴³ P. Werner, A. J. Millis, Phys. Rev. Lett. **104**, 146401 (2010).
 - ⁴⁴ C. Friedrich, S. Blügel, and A. Schindlmayr, Phys. Rev. B **81**, 125102 (2010). <http://www.flapw.de/>.
 - ⁴⁵ N. Marzari and D. Vanderbilt, Phys. Rev. B **56**, 12847 (1997).
 - ⁴⁶ I. Souza, N. Marzari, and D. Vanderbilt, Phys. Rev. B **65**, 035109 (2001).
 - ⁴⁷ R. Sakuma, Phys. Rev. B **87**, 235109 (2013).
 - ⁴⁸ A. A. Mostofi, J. R. Yates, Y.-S. Lee, I. Souza, D. Vanderbilt, and N. Marzari, Comput. Phys. Commun. **178**, 685 (2008).
 - ⁴⁹ F. Aryasetiawan, M. Imada, A. Georges, G. Kotliar, S. Biermann, and A. I. Lichtenstein, Phys. Rev. B **70**, 195104 (2004).
 - ⁵⁰ A fully self-consistent GW+DMFT treatment, beyond the scope of this work, may lead to modifications in the balance between local and nonlocal correlations.⁵¹
 - ⁵¹ T. Ayril, S. Biermann, and P. Werner, Phys. Rev. B **87**, 125149 (2013).
 - ⁵² M. Casula, Ph. Werner, L. Vaugier, F. Aryasetiawan, T. Miyake, A. J. Millis, and S. Biermann Phys. Rev. Lett. **109**, 126408 (2012).